Journal of the Professional Association for Cactus Development

Formation of calcium oxalates and carbonates due to water stress in "nopalitos"

Rafael Zuñiga-Valenzuela[1], Edgar Vladimir Gutiérrez-Castorena[2‡], Ma. Del Carmen Gutiérrez-Castorena[3], Elizabeth Zuñiga-Valenzuela[1], Edgar Miguel García-Carrillo[4]

[1]Facultad de Agricultura y Zootecnia, Universidad Juárez del Estado de Durango. Carretera Gómez Palacio-Tlahualilo Km 32, Venecia, Gómez Palacio, Durango 35000. México.
[2]Facultad de Agronomía, Universidad Autónoma de Nuevo León, Francisco I. Madero S/N, Ex. Hacienda el Canadá, General Escobedo 66050, México.
[3]Programa de Edafología, Colegio de Postgraduados, Carretera México-Texcoco km 36.5 Montecillo, Texcoco 56230, México.
[4] Centro de Investigación en Química Aplicada, Enrique Reyna H. 140, San José de los Cerritos, 25294 Saltillo, Coahuila, México.

‡Corresponding author: edgar.gutierrezcs@uanl.edu.mx.

Abstract. The "nopalitos" (*Opuntia ficus-indica* L. Miller) is an essential source of calcium in the human diet; however, the bioavailability and viability of the mineral are limited by precipitating in the form of calcium oxalate (CaC_2O_4) when the plant is exposed to water stress. The objective of this study was to quantify calcium oxalates and carbonates in cactus subjected to water differentials of 10, 30 and 60% of available water (AW) through photomicrographic analysis. The micro mosaics are composed of sequential images of a 10x amplitude, taken in a petrographic microscope with different light sources, plane-polarized light (LPP), cross-polarized light (LPC), and light compensated (LPC). High spectral resolution mosaics were produced using geospatial operators (ArcGIS v.10.1 and ERDAS Imagine, 2014v®). The CaC_2O_4 and $CaCO_3$ were identified by spectral signature or brightness degrees in RGB format images, quantifying the minerals and surface they occupy in the cladode. The quantification of minerals *in situ* in nopal cladodes at different water stresses showed significant differences ($p<0.05$) in the area occupied by oxalates at 10% water stress and calcium carbonates at 60% within the vegetal structures of nopal vegetables. Consequently, using high-resolution mosaics and spatial operators allows the identification and quantification of mineral biomarkers in plant tissues *in situ*. Therefore, using image overlay, the proposed method is an alternative to the *in situ* quantification of minerals in plant tissues.

Key words: Micro mosaics, in situ, image overlay, water stress, calcium oxalates, calcium carbonates.

Cite: Zuñiga-Valenzuela, R, Gutiérrez-Castorena, E.V., Gutiérrez-Castorena, M.C., Zuñiga-Valenzuela, E. and García-Carrillo, E. 2024. Formation of calcium oxalates and carbonates due to water stress in nopal vegetables. *Journal of the Professional Association for Cactus Development. 26*:43-57. https://doi.org/10.56890/jpacd.v26i.553.

Guest Editor: José Luis García-Hernández.

Technical Editor: Benjamin Hernández Vázquez.

Received date: 20 January 2024
Accepted date: 03 March 2024
Published date: 08 April 2024

Introduction

Due to inorganic substances originated by living organisms, calcium carbonate ($CaCO_3$) is an abundant compound in cactus, an important aspect in the development of new fields of application (Shu-Chen *et al*.,

2007). In Mexico, the contribution of calcium in the diet of the population is mainly reduced to the consumption of dairy products due to the limited information on the content of this mineral in different foods. However, the nopal vegetable serves as an alternative due to its high calcium content, in addition to being a viable product due to its availability and accessibility in different regions of the country (Heaney, 2001; Fairweather, 2007; Moran *et al.,* 2013).

However, this element is only available in high nutritional concentrations, such as oxalic acid ($C_2H_2O_4$) or dietary fiber (Kennefick and Cashman, 2000; Heaney, 2001; Charoenkiatkul *et al*., 2008), preventing its absorption by being sequestered as calcium oxalates, with a variability between 8 and 50% of the dry weight of the cladode (Gallaher, 1975; McConn and Nakata, 2004). Likewise, the consumption of nopalitos varies depending on the state of ripeness (between 400 and 500 g), showing high levels of oxalate-free calcium (3.4 g in 100 g).

It has been documented that the concentration of Ca^{++} increases at different stages of maturation of the cladodes (17.9 at 40 days and 34.4% at 135 days) (Contreras-Padilla *et al*., 2011). However, its availability decreases because it is bound by oxalate, which interferes with the precipitation and toxicity of oxalic acid (Franceschi and Loewus, 1995). The latter acts as a nutrient store in response to water or nutritional stress (Kostman *et al*., 2001).

According to Franceschi and Horner (1980), due to the physiology of the cactus, four types of calcium oxalate crystals are produced, classified according to their morphology, raphides (acicular crystals in aggregates), druses (spherical crystalline aggregates), styloids (acicular crystals) and prisms.

The morphology and distribution of the crystals resemble whewellite (calcium oxalate monohydrate) or weddellite (calcium oxalate dihydrate) (Franceschi and Horner, 1980) which has established a direct relationship between the formation and size of plant tissues as a function of stress by dehydration (star-shaped tetragonal weddellite) (Zuñiga-Valenzuela *et al*., 2018; Monje and Baran, 2002) compared to calcium carbonates, where pressure and temperature conditions modify their shape, giving rise to monohydrated or cubic calcium carbonate minerals in plant species (Zuñiga-Valenzuela *et al*., 2018; Young *et al*., 2003; Franceschi and Horner, 1980).

The calculation and analysis of the spatial distribution of calcium oxalates and carbonates in cladodes is challenging because conventional methods of plant tissue micromorphology at different scales are qualitative, which originates a greater margin of error when comparing the data (McBratney *et al*., 2000) even within a single thin section. Hence the proposal is to study them under soil micromorphological techniques as it is an effective tool that allows analyzing samples in place without alteration and serves as an alternative for plant analysis that allows quantifying and analyzing the spatial distribution of minerals in the cladodes (Jangorzo *et al*., 2014).

Currently, mineral analysis is performed individually and with discrete images (Adderley *et al*., 2002; Aydemir *et al*., 2004; Poch and Virto, 2014) or with images of different spectral resolution. This type of analysis limits the amount of information about interactions or relationships between plant components and their mineral characteristics that can be obtained from thin sections at different micro scales (Van den Bygaart and Protz, 1999). For example, aggregates and plant residues (Zaiets and Poch, 2016). Because of this, Bryk (2016) recommends the use of flatbed scanners to provide an overview of the spatial distribution of pedofeatures in plant tissue.

https://www.jpacd.org Electronic ISSN: 1938-6648

Quantitative spatial analysis of mosaics in thin sections comprises a surface area ranging from 1,643 to 5,575 mm² (Dorronsoro, 2015), with a high spatial resolution of 5.3-micron pixel (Sauzet *et al*., 2017). However, this ability is limited by the absence of a coordinate system, that is, it is impossible to superimpose images with different formats (either raster or vector). Consequently, the location of the minerals in the cladode space cannot be determined exactly, which makes it difficult to establish relationships between the fundamental components (Gutiérrez-Castorena *et al*., 2018). To achieve this, geographic information systems (GIS) allow the processing of high-resolution mosaics with reference images (Terribile and Fitzpatrick, 1995; Tarquini and Favalli, 2010), identifying the elements of interest by using three types of light (flat, cross, and offset) by mapping and overlaying the identified components (Gutiérrez-Castorena *et al*., 2016).

The methods to characterize calcium oxalates and carbonates in cladodes require very specific and expensive instruments, such as scanning electron microscopy coupled to a dispersive X-ray spectrometer (EDS). Other studies (Monje and Baran, 2002) have used systematic infrared spectroscopy to analyze the chemical nature of crystals. The characterization of calcium oxalate drusen in plant tissue (Monje and Baran, 2002), as well as the characterization of mineral inclusion cells, the chemical composition and their morphology through identification by X-ray diffraction (XRD) and petrographic microscope (Bárcenas-Argüello *et al*., 2015).

The objective of this study was to implement a methodology to identify and quantify the geospatial distribution of calcium oxalates and carbonates within the cactus plant structures at different levels of water stress through a micromorphological analysis in thin sections, as a viable alternative for analysis using transmission microscopy (Tarquini and Favalli, 2010; Gutiérrez-Castorena *et al*., 2016). In addition, it has been established that water stress favors the formation of calcium oxalates in nopal, so that the evaluation of available water levels will allow determining the crystalline system of both calcium carbonate (calcite) and calcium oxalate, through the analysis of digital mosaics of high spatial and spectral resolution, with dichromometric and densitometric parameters in plant tissues.

Material and Methods

The study was carried out between the coordinates 25° 52' 35" N and 100° 1' 41" W. The experimental units were established in containers 36 cm high, 28.5 cm in diameter and with a volume of 23.6 cm³ under conditions controlled. The plant material “nopalitos” (young plant stems) were extracted from experimental plots of the Facultad of Agricultura of the Universidad Autónoma of Nuevo León, Monterrey, México. The variety was Villa Nueva planted after sanitary treatment.

The nopal was subjected to water stress, which consisted of reducing the amount of available water by 60, 30 and 10% based on the volume of the container (Figure 1), taking as reference the field capacity and point of permanent wilt of the substrate. The irrigation was determined based on the periodic weight of the pots until the required humidity levels were reached.

The irrigations were determined based on the periodic weight of the pots until reaching the required humidity levels.

https://www.jpacd.org Electronic ISSN: 1938-6648

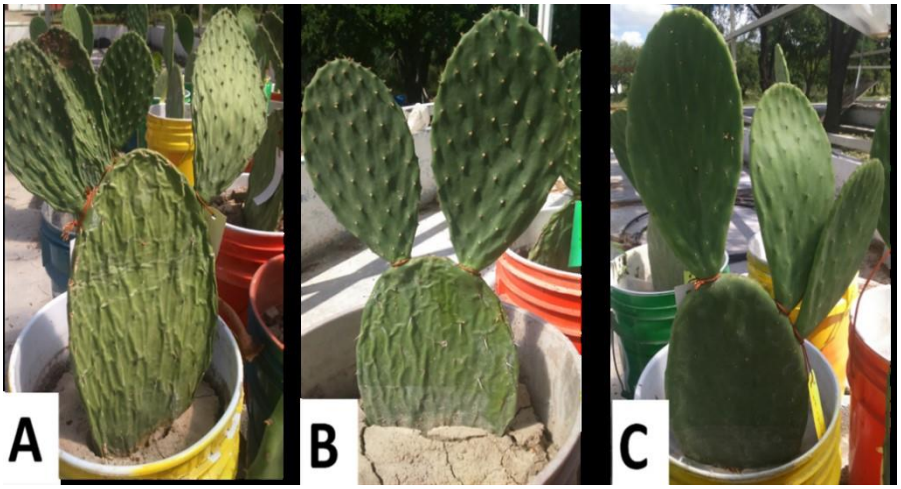

Figure 1. Vegetal state of the cladodes according to the corresponding available water treatment. A) 10, B) 30 and C) 60%.

The experimental design was a randomized block with three replications; plant tissue samples were obtained from a cladode per replicate at 60 days of maturation and were subjected to a dehydration with 100% of acetone (CH_3CH_3) for 30 days, impregnated with 90% resin and styrene monomer (C_8H_8) to 10%.

The impregnation was carried out in a vacuum chamber for 45 minutes at 35 lb. tension, drying for 15 days at room temperature in shaded conditions. The dry samples were divided into 5 zones (Figure 2), later they were cut and placed on coverslips. They were fixed with epoxy resin and polished to a thickness of 30 µm, taking 1 cm² from the center of each repeat.

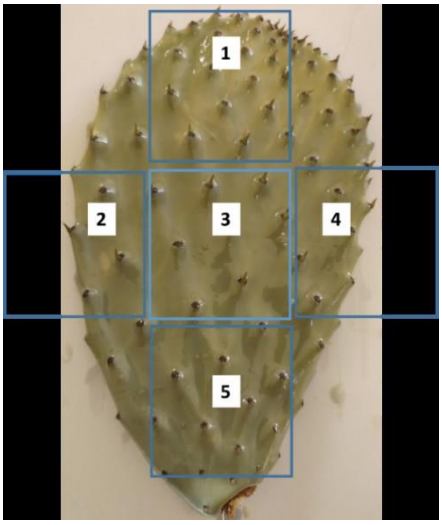

Figure 2. Sampling areas in the cladode.

The original mosaic was made from the micromorphological analysis (Figure 3A), which consisted of capturing sequential micro images with different light sources at a 10× objective, using a digital camera mounted on a petrographic microscope (Olympus BX51). Subsequently, high spatial resolution micro-photomosaics were created, making a 1 cm² cutout (Figure 3). Likewise, microscale approximations were made to carry out the map algebra and the respective thematic maps for the observation and

https://www.jpacd.org Electronic ISSN: 1938-6648

classification of calcium oxalates, calcium carbonates, empty space and plant tissue residues, using colors to facilitate their identification and avoid confusion when classifying the different minerals of interest. Image analysis was performed using the ERDAS Imagine 2014v® software.

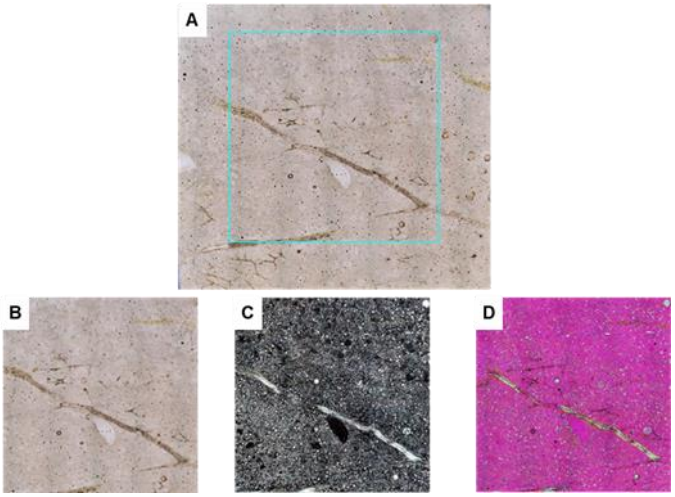

Figure 3. A) Original mosaic of plant tissue component, 1 cm^2 cuts. A) flat light, B) flat light, C) crossed light, and D) polarized light.

The processes for the quantification of calcium oxalates and carbonates were based on the methodology reported by Gutiérrez-Castorena *et al*. (2016) by converting raster information into vector format using ArcGis v.10.1. The study consisted of observing the area where the oxalates and calcium carbonates are concentrated in the cladode, taking three random micro-photographs per zone, and a second analysis, which consists of counting the cladode sampled zones to obtain the area treated by the different minerals, and perform a comparison of means using Tukey's method, with a significance level of $p \leq 0.05$.

Results and Discussion

The micro cartography located and identified the oxalates and calcium carbonates with a visual magnification of the mosaics (Figure 4) at a scale of 4.5 and an area of 2.4 mm^2, to observe the characteristics of each mineral, like reported by Gutiérrez-Aguilar (2012), and identification of calcium oxalates in microphotographs with a zoom of 50× to 500× and calcium carbonates from 1000× to 3500×.

According to Contreras-Padilla *et al*. (2011) the calcium oxalates in the nopal appear in the form of a druse, like observed in the mosaic with polarized light (orange color); While the calcium carbonates showed a grouped sequence (blue color) and in the form of cubes (figures 4 and 5), as indicated by Gutiérrez-Aguilar (2012).

https://www.jpacd.org Electronic ISSN: 1938-6648

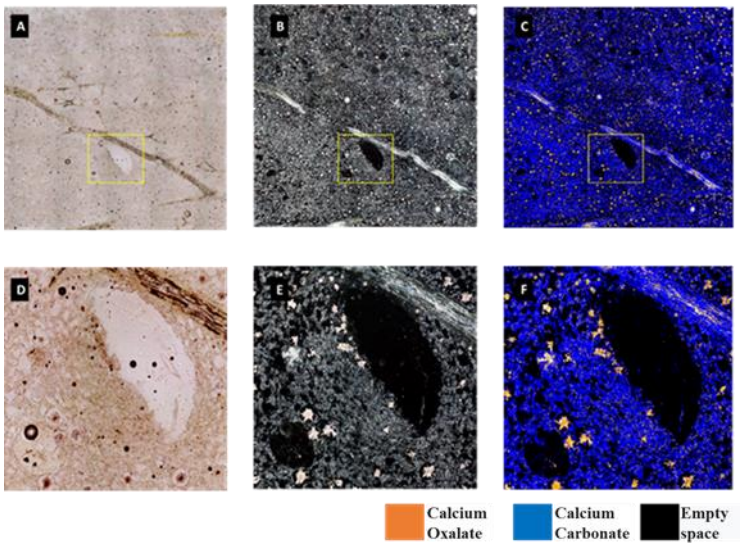

Figure 4. Thematic maps of components in plant tissue at a real visible field of 1 cm^2. A) flat light; B) cross light; C) thematic map of minerals; Mosaic magnification to a scale of 86:1 and area of 2.4 mm^2. D) flat light; E) cross light; F) thematic map of minerals.

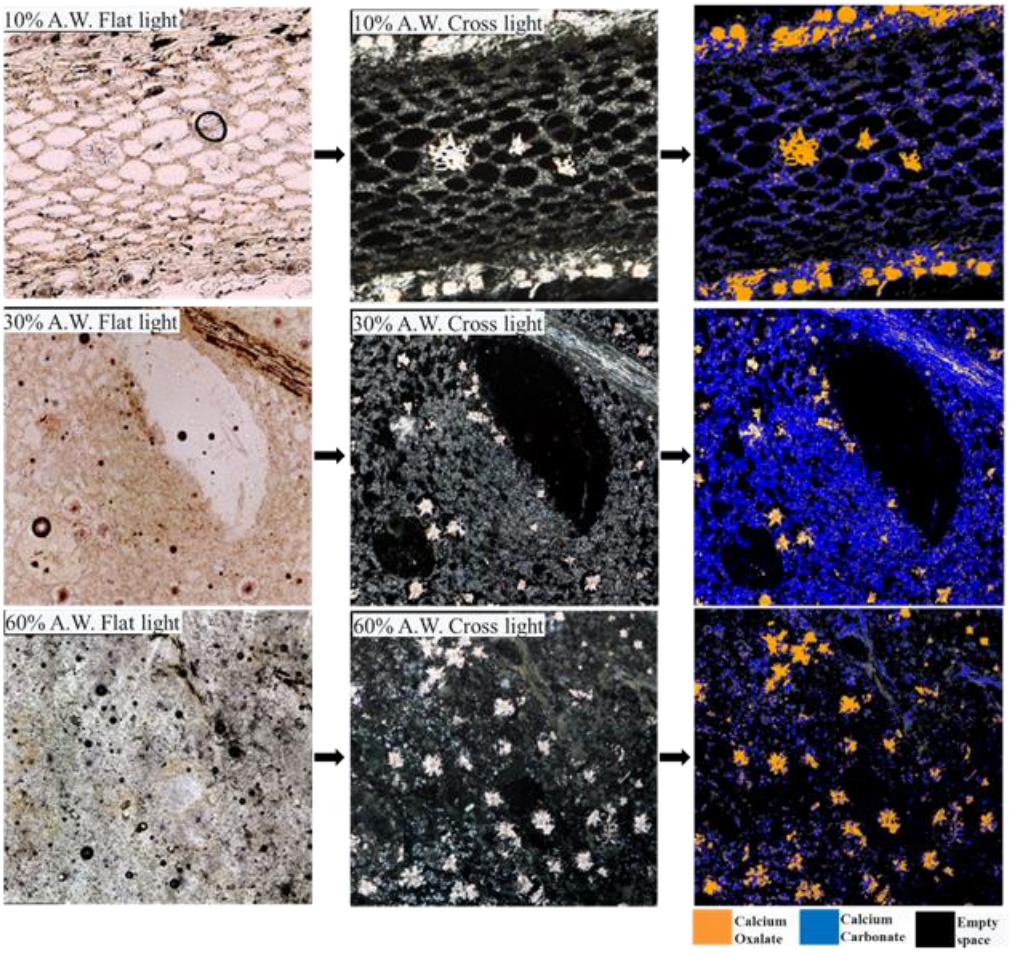

Figure 5. Visual enlargement of the thematic maps of distribution of calcium oxalates and carbonates in plant tissue of the water treatments 10, 30 and 60% of available water (AW), at a scale of 86:1 and an area of 2.4 mm^2.

https://www.jpacd.org Electronic ISSN: 1938-6648

Calcium oxalates are produced in the mucilaginous cells of the nopal cactus by concentrating the greatest amount of organic and inorganic acids on the collenchyma in the form of tetragonal weddellite (star shape) and are distributed on the cell wall due to the movement of calcium within the plant passively (Rodríguez-García *et al*., 2007). On the other hand, all calcium carbonate crystals are micritic, indicating rapid precipitation due to changes in CO_2, while oxalate crystals are larger, implying slow development. This development phenomenon is attributed to the state of hydration of the cladode and its maturation time due to the concentration of malic and ascorbic acids.

The quantification and placement of calcium oxalates and carbonates in plant structures were achieved by separating the minerals through a supervised classification with polygons or vector layers, according to the methodology described by Gutiérrez-Castorena *et al*. (2016) (Figure 6).

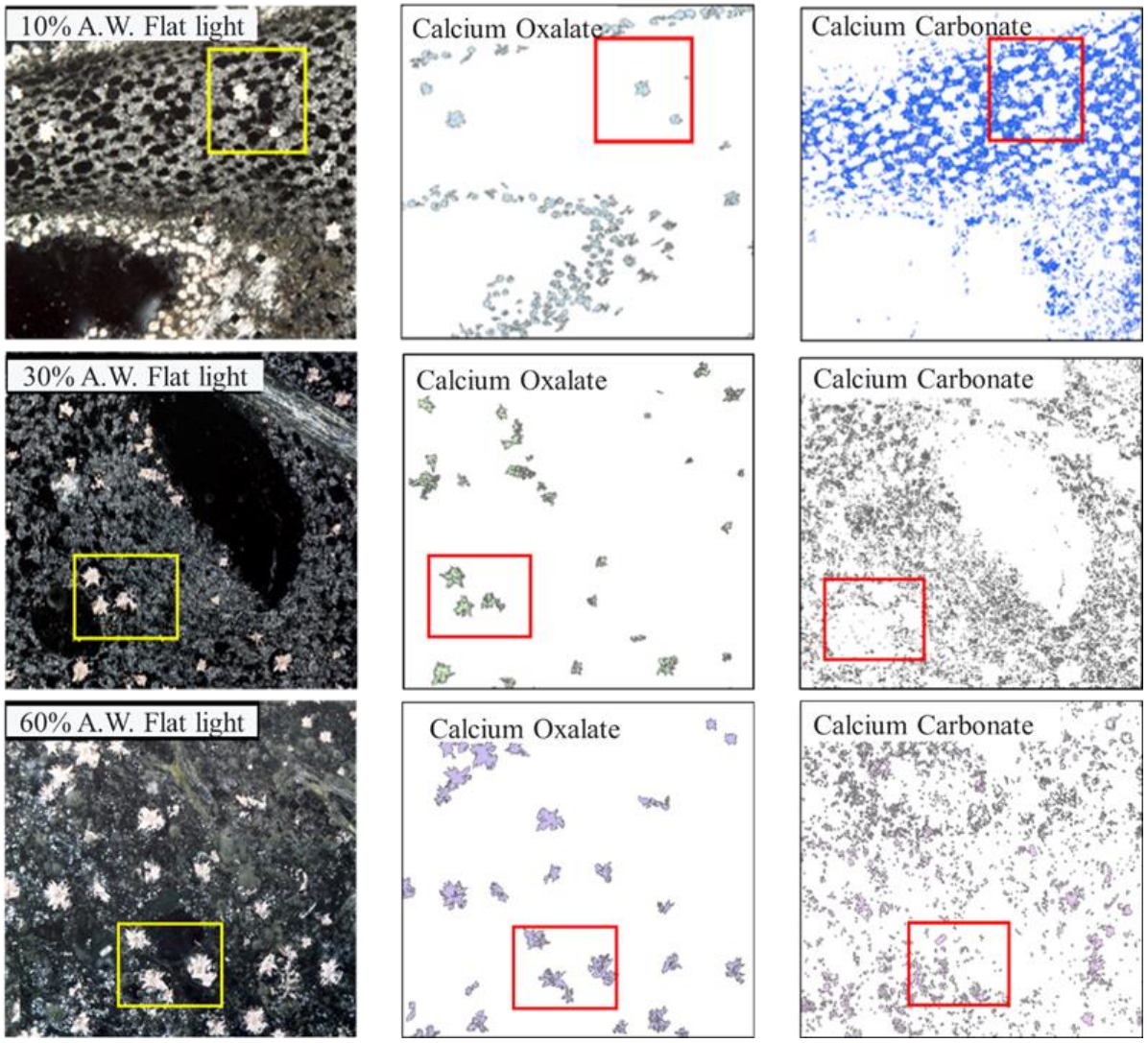

Figure 6. Thematic maps of calcium oxalates and calcium carbonate in plant tissue at 10%, 30% and 60% available water in crossed light and vector extraction of polygons at 86:1 scale and 2.4 mm^2 area.

The number of polygons of calcium oxalates (Table 1) showed a significant difference ($p \leq 0.01$) between treatments, observing a higher concentration in the treatment at 10% of available water

https://www.jpacd.org Electronic ISSN: 1938-6648

(6,409), while the treatments of 30 and 60% of available water showed concentrations of 3,441 and 1,499, respectively (Figure 7).

Table 1. Analysis of variance at different amounts of available water on the presence of calcium oxalates and calcium carbonates.

Concentration of calcium oxalates and calcium carbonates	DF	Mean squares
Calcium oxalates	2	30573740.0**
Calcium Carbonates	2	38017.2*

** p=0.01 y * p=0.05, DF= Degrees of freedom.

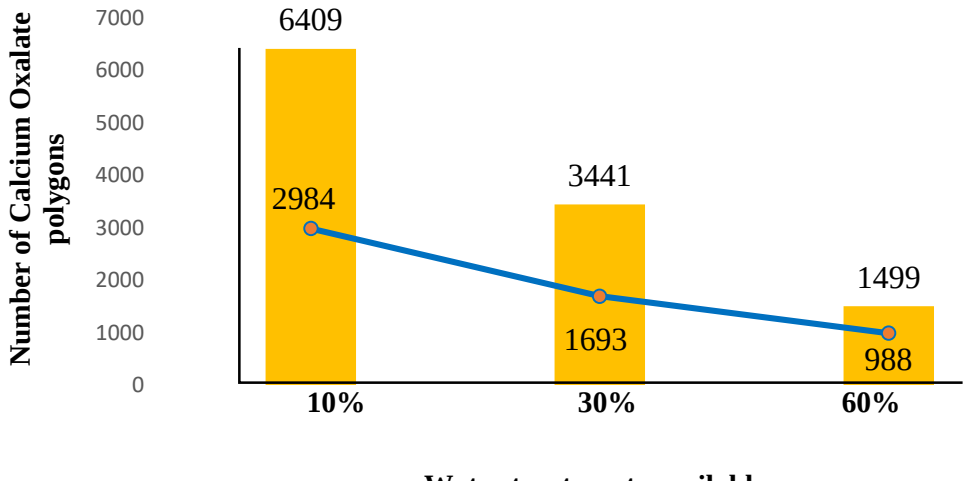

Figure 7. Quantification of calcium oxalates in different water stresses of the cladode (the line shows the standard deviation).

Likewise, water stress had an influence on the formation and distribution of the mineral, with a significant difference (p≤0.05) between zones 2 and 4 (Table 2). This higher concentration was observed in the 10% AD treatment. The treatments with 10 and 30% AD showed a higher frequency of minerals in zone 4, with concentrations of 628 and 208, respectively; while in the treatment with 60% available water, a greater amount of calcium oxalate polygons was found in zone 3, with 97 minerals (Figure 8).

Table 2. Analysis of variance of the concentration of Calcium Oxalates in the cladode zones

Concentration of calcium oxalates by zone of the cladode	DF	Mean squares
10% water available	4	132,343.9*
30% water available	4	10,789.6
60% water available	4	2,761.8

** p=0.01 y * p=0.05, DF= Degrees of freedom.

https://www.jpacd.org Electronic ISSN: 1938-6648

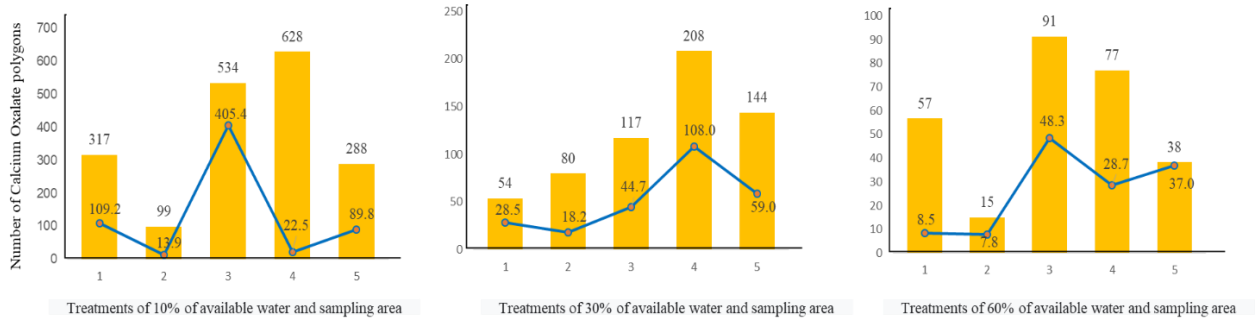

Figure 8. Quantification of calcium oxalate polygons by sampling area at 10, 30 and 60% of available water (The line shows the standard deviation).

On the other hand, the concentration of calcium carbonates showed a significant difference ($p \leq 0.05$) between treatments (Table 1) with a concentration of 206.5 mg cm^{-3} in the treatment of 60% AW, with a greater quantity in zone 4 with 3.6 and 13.1 mg cm^{-3}, contrary to the 10% treatment, showing a greater quantity in zone 2 with 2.4 mg cm^{-3}; however, did not show significant difference between zones (Figure 10).

Table 3. Analysis of variance of the concentration of calcium oxalates in the cladode zones.

Concentration of calcium carbonates by zone of the cladode	DF	Mean squares
10% water available	4	1.55
30 % water available	4	4.02**
60 % water available	4	12.5**

** p=0.01 y * p=0.05, DF= Degrees of freedom.

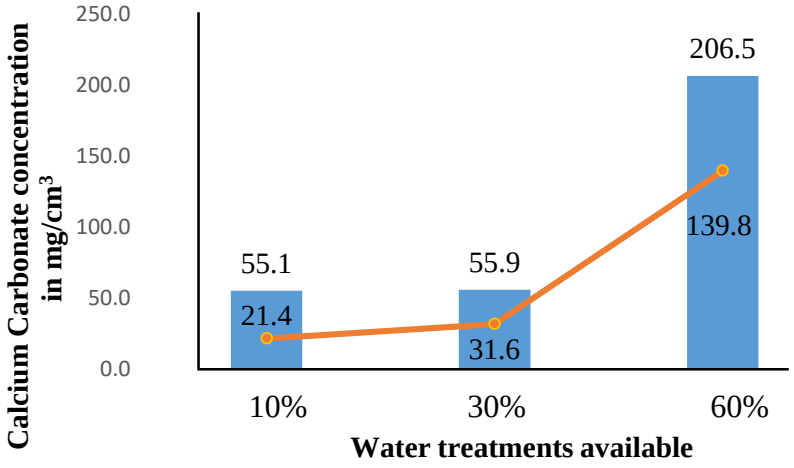

Figure 9. Concentration (mg cm^{-3}) of calcium carbonates at different water stress of the cladode (the line shows the standard deviation).

https://www.jpacd.org Electronic ISSN: 1938-6648

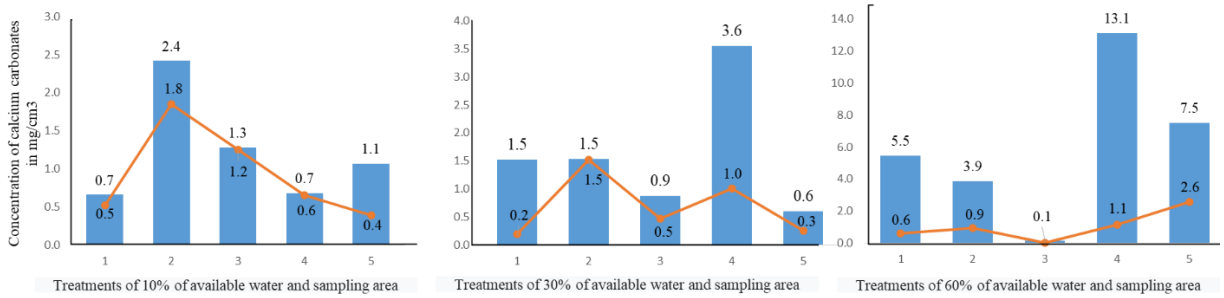

Figure 10. Concentration (mg cm^{-3}) of calcium carbonates by sampling zone at 10, 30 and 60% of available water (the line shows the standard deviation).

The different techniques used to characterize the crystals of oxalate and calcium carbonates, such as chemical analysis, X-ray diffraction, petrography, scanning electron microscope, are limited due to the destructive method of plant tissue (Monje and Baran, 2003; Moje and Baran, 2009; Bárcenas *et al*., 2015). However, the use of micro morphometry in thin sections in situ samples seems to be an alternative to obtain real quantification on plant tissues and identification of minerals such as calcium oxalate and carbonate.

Conclusions

The water stress in nopal cultivation has an influence on the size, quantity, and shape or distribution of calcium oxalates and carbonates found in plant structures at 60 days of maturation. Dichromorphometric and densitometric analyzes allow the identification and characterization of unaltered cladode samples subjected to different levels of water stress (10, 30 and 60% of available water), so that the proposed method is an alternative for the *in situ* quantification of minerals. in plant tissues.

ETHICS STATEMENT

Not applicable

CONSENT FOR PUBLICATION

Not applicable

COMPETING INTEREST

The authors declare that they have no competing interests.

AVAILABILITY OF SUPPORTING DATA

All data generated or analyzed during this study are included in this published paper.

COMPETING INTERESTS

The authors declare that they have no competing interests.

AUTHOR CONTRIBUTION

Conceptualization, Z.V-R., G.C-E.V. Methodology, G.C-M.C., G.C-E.V., Z.V-R, Validation, Z.V-R., G.C-E.V. Formal analysis, G.C-M.C., G.C-E.V. Research, G.C-M.C., G.C-E.V., Z.V-R. Resources, Z.V-R., Z.V-E. Visualization, Z.V-R., G.C-E.V. Literature review, Z.V-E. Supervision G.C-M.C. review of the final version and approval of the manuscript before sending it, G.C-M.C., G.C-E.V., Z.V-R., Z.V-E.

ACKNOWLEDGEMENTS

Thanks to the Faculty of Agronomy of the Universidad Autonóma de Nuevo Leon and the Soil Science Program, Colegio of Postgraduados.

References

Adderley, W.P., Simpson, I.A. and Davidson, D.A. 2002. Colour description and quantification in mosaic images of soil thin Section. *Geoderma. 108:*181–195. https://doi.org/10.1016/S0016-7061(02)00123-4

Aydemir, S., Keskin, S. and Creés, L.R. 2004. Quantification of soil features using digital image processing (DIP) techniques. *Geoderma. 119:*1-8. https://doi.org/10.1016/S0016-7061(03)00218-0

Bárcenas-Argüello, M.L., Gutiérrez-Castorena, M.C.D.C. and Terrazas, T. 2015. Los cristales polimórficos de weddellita en tres especies de Cephalocereus (Cactaceae). *Micron*. *77*:1-8. https://doi.org/10.1016/j.micron.2015.05.014

Bryk, M. 2016. Macrostructure of diagnostic B horizons relative to underlying BC and C horizons in Podzols, Luvisol, Cambisol, and Arenosol evaluated by image analysis. *Geoderma*, *263:*86-103. https://doi.org/10.1016/j.geoderma.2015.09.014

Charoenkiatkul, S., Kriengsinyos, W., Tuntipopipat, S., Suthutvoravut, U. and Weaver, C.M. 2008. Absorción de calcio de vegetales de consumo común en mujeres tailandesas sanas. *Revista de Ciencia de los Alimentos*. *73*(9):H218-H221. https://doi.org/10.1111/j.1750-3841.2008.00949.x

Contreras-Padilla, M., Pérez-Torrero, E., Hernández-Urbiola, M.I., Hernández-Quevedo, G., del Real, A., Rivera-Muñoz, E.M. and Rodríguez-García, M.E., 2011. Evaluación de oxalatos y calcio en yemas de nopal (*Opuntia ficus-indica* var. redonda) en diferentes estados de madurez. *Diario de Composición y Análisis de Alimentos*. *24*(1):38-43. https://doi.org/10.1016/j.jfca.2010.03.028

Dorronsoro, C. 2015. *Giga-images. The Scanned Images of the Walter Kubiëna Collection* [WWW document]. URL http://www.edafologia.net/micropano/index_en.html [accessed on 12 April 2016].

Fairweather-Tait, S.J. and Teucher, B. 2002. Biodisponibilidad del calcio en relación con la salud ósea. *Revista Internacional de Investigación sobre Vitaminas y Nutrición*. *72:*13-18.

Franceschi, V.R. and Loewus, F.A. 1995. Oxalate biosynthesis and function in plants. In: Khan, S.R. (ed.). Calcium oxalate in biological systems, FL. *pp*:113-130.

Franceschi, V.R. and Horner, H.T. 1980. Cristales de oxalato de calcio en plantas. *La Revista Botánica*. *46*:361-427.

Gallaher, R.N. 1975. The occurrence of calcium in plant tissue as crystals of calcium oxalate. *Communications in Soil Science and Plant Analysis*. *6*(3)*:*315-330. https://doi.org/10.1080/00103627509366570

Gutiérrez-Aguilar, L. 2012. Identificación de compuestos de calcio en cladodios de nopa*l (Opuntia ficus indica)*. https://ri-ng.uaq.mx/handle/123456789/6714

Gutiérrez-Castorena, E.V., Gutiérrez-Castorena, M.d.C., González-Vargas, T., Cajuste, B.L., Delgadillo, M.J. and Suástegui, M.E. 2016. Micromapping of microbial hotspots and biofilms from different crops using digital image mosaics and soil thin sections. *Geoderma*. *279:*11–21. https://doi.org/10.1016/j.geoderma.2016.05.017

Gutiérrez-Castorena, M.C., Gutiérrez-Castorena, E.V., González-Vargas, T., Ortiz-Solorio, C.A., Suástegui-Méndez, E., Cajuste-Bontemps, L. and Rodríguez-Mendoza. M.N. 2018. Thematic micro-aps of soil components using high-resolution spatially referenced mosaics from whole soil thin sections and image analysis. *European Journal of Soil Science*. *69:*217-231. https://doi.org/10.1111/ejss.12506

Heaney, R.P. 2001. Meta-analysis of calcium bioavailability. *American Journal of Therapeutics*. *8(1):* 73.

Jangorzo, N.S., Schwartz, C. and Watteau, F. 2014. Image analysis of soil thin sections for a non-destructive quantification of aggregation in the early stages of pedogenesis. *European Journal of Soil Science*. *65:* 485–498. https://doi.org/10.1111/ejss.12110

Kennefick, S. and Cashman, K.D. 2000. Inhibitory effect of wheat fibre extract on calcium absorption in Caco-2 cells: evidence for a role associated phytate rather than fibre per se. *European Journal of Nutrition. 39:*12-17.

Kostman, T.A., Tarlyn, N.M., Loewus, F.A. and Franceschi, V.R. 2001. Biosynthesis of L-ascorbic acid and conversion of carbons 1 and 2 of L-ascorbic acid to oxalic acid occurs within individual calcium oxalate crystal idioblasts. *Plant Physiology*. *125*(2)*:* 634-640. https://doi.org/10.1104/pp.125.2.634

McBratney, A.B., Odeh, I.O., Bishop, T.F., Dunbar, M.S. and Shatar, T.M., 2000. An overview of pedometric techniques for use in soil survey. *Geoderma*. *97:*293–327. https://doi.org/10.1016/S0016-7061(00)00043-4

McConn, M.M. and Nakata, P.A. 2004. Oxalate reduces calcium availability in the pads of the prickly pear cactus through formation of calcium oxalate crystals. *Journal of Agricultural and Food Chemistry*. *52:*1371-1374. https://doi.org/10.1021/jf035332c

Monje, P.V. and Baran, E.J. 2002 Characterization of calcium oxalates generated as biominerals in cacti. *Plant Physiology*. *128:*707-713. https://doi.org/10.1104/pp.010630

Moran, S., Mina. A., Duque, J., Anaya, S., San-Martin, U., Yañez, P. and Leal, R.G. 2013. Prevalence of lactose malabsorption in Mexican children: importance of measuring methane in expired air. *Medical Research Archives*. *44*(4):291-295. https://doi.org/10.1016/j.arcmed.2013.04.005

Payne, S. R., Heppenstall-Butler, M. and Butler, M.F. 2007. Formation of thin calcium carbonate films on chitosan biopolymer substrates. *Crystal Growth and Design*. *7*(7)*:*1262-1276. https://doi.org/10.1021/cg060687k

Poch, R.M. and Virto, I. 2014. Micromorphology techniques for soil organic carbon studies. In: *Soil Carbon, Progress in Soil Science.* Eds. Hartemink, A.E. and McSweeney, K. 17-26 pp. Springer International Publishing, Cham, Switzerland. https://doi.org/10.1007/978-3-319-04084-4_2

Rodríguez-García, M.E., De Lira, C., Hernández-Becerra, E., Cornejo-Villegas, M.A., Palacios-Fonseca, A.J., Rojas-Molina, I. and Muñoz-Torres, C. 2007. Physicochemical characterization of nopal pads (*Opuntia ficus indica*) and dry vacuum nopal powders as a function of the maturation. *Plant Foods for Human Nutrition*. *62:*107-112. https://doi.org/10.1007/s11130-007-0049-5

Sauzet, O., Cammas, C., Guilliot, J.M., Bajard, M. and Montagne, D. 2017. Development of a novel image analysis procedure to quantify biological porosity and illuvial clay in large thin sections. *Geoderma*. *292:*135-148. https://doi.org/10.1016/j.geoderma.2017.01.004

Shu-Chen, H., Kensuke, N. and Yoshiki, C. 2007. A carbonate controlled-addition method for amorphous calcium carbonate spheres stabilized by poly (acrylic acids). *Langmuir. 23:*12086-12095. https://doi.org/10.1021/la701972n

Tarquini, S. and Favalli, M. 2010. A microscopic information system (MIS) for petrographic analysis. *Computers and Geosciences*. *36:*665-674. https://doi.org/10.1016/j.cageo.2009.09.017

Terribile, F. and Fitzpatrick, E.A. 1995. The application of some image-analysis techniques to recognition of soil micromorphological features. *European Journal of Soil Science*. *46:*29-45. https://doi.org/10.1111/j.1365-2389.1995.tb01810.x

Van den Bygaart, A.J. and Protz, R. 1999. The representative elementary area (REA) in studies of quantitative soil micromorphology. *Geoderma*. *89:*333-346. https://doi.org/10.1016/S0016-7061(98)00089-5

Young, J., Geisen, M., Cros, L., Kleijne, A., Sprengel, C., Probert, I. and Ostergaard, J., 2003. A guide to extant coccolithophores taxonomy. *Journal of Nannoplankton Research*. *1:*125.

Zaiets, O. and Poch, R.M. 2016. Micromorphology of organic matter and humus in Mediterranean mountain soils. *Geoderma*. *272:*83-92. https://doi.org/10.1016/j.geoderma.2016.03.006

Zuñiga-Valenzuela, R., Gutiérrez-Castorena, Ma. C., Gutiérrez-Castorena, E.V., Olivares-Sáenz, E., Méndez-Gallegos, S.D.J., Carranza-de la Rosa, R., and Vázquez-Alvarado, R.E. 2018. Caracterización $CaCO_3$ y CaC_2O_4 con análisis microfotográfico en *Opuntia ficus-indica* (L.) Miller. *Revista Mexicana de Ciencias Agrícolas*. *9:*7.